Insertion of Telomere Repeat Sequence Decreases Plasmid DNA Condensation by Cobalt (III) Hexaammine

Jason R. Schnell,* Judith Berman,# and Victor A. Bloomfield*
Departments of *Biochemistry and #Plant Biology, University of Minnesota, St. Paul, Minnesota 55108

ABSTRACT Telomere repeat sequence (TRS) DNA is found at the termini of most eukaryotic chromosomes. The sequences are highly repetitive and G-rich (e.g., $[C_{1-3}A/TG_{1-3}]_n$ for the yeast *Saccharomyces cerevisiae*) and are packaged into nonnucleosomal protein-DNA structures in vivo. We have used total intensity light scattering and electron microscopy to monitor the effects of yeast TRS inserts on in vitro DNA condensation by cobalt (III) hexaammine. Insertion of 72 bp of TRS into a 3.3-kb plasmid depresses condensation as seen by light scattering and results in a 22% decrease in condensate thickness as measured by electron microscopy. Analysis of toroidal condensate dimensions suggests that the growth stages of condensation are inhibited by the presence of a TRS insert. The depression in total light scattering intensity is greater when the plasmid is linearized with the TRS at an end (39–49%) than when linearized with the TRS in the interior (18–22%). Circular dichroism of a 95-bp fragment containing the TRS insert gives a spectrum that is intermediate between the A-form and B-form, and the anomalous condensation behavior of the TRS suggests a noncanonical DNA structure. We speculate that under conditions in which the plasmid DNA condenses, the telomeric insert assumes a helical geometry that is similar to the A-form and is incompatible with packing into the otherwise B-form lattice of the condensate interior.

INTRODUCTION

Packaging of DNA into compact, regular structures occurs in virtually all organisms. This packaging results from the need to efficiently and reversibly package the long linear polymer into a small compartment. DNA can have packing ratios on the order of 10^3 in viral capsids and prokaryotes, and on the order of 10^5 in metaphase eukaryotic chromosomes. A regular high-density toroidal structure similar to that seen in lysed viral capsids can be obtained in a test tube containing only DNA suspended in a dilute aqueous buffer solution of cationic polyamines (Gosule and Schellman, 1976). Over the past two decades, much work has gone into characterizing the effects of DNA concentration (Widom and Baldwin, 1980; 1983), size and topology (Arscott et al., 1990; Ma and Bloomfield, 1994), condensing agent structure (Plum et al., 1990; Thomas and Bloomfield, 1984), and solution conditions (Arscott et al., 1995; Duguid et al., 1995; Thomas and Bloomfield, 1983; Widom and Baldwin, 1980; Wilson and Bloomfield, 1979) on the DNA condensation process (for a recent review, see Bloomfield, 1996).

A more recent development is the finding that DNA sequence and secondary structure play a role in determining the extent and morphology of the DNA condensates. Minsky's group has condensed DNA fragments containing intrinsically bent A-tracts and observed the formation of regular toroids, but with an unusually small inner radius of curvature (Reich et al., 1992). Studies on sequences capable of undergoing the B- to Z-DNA transition indicate that these DNAs have an enhanced condensability (Ma et al., 1995). Furthermore, poly(dG-dC) · poly(dG-dC) can assume distinct condensate morphologies with a complex dependence on condensing agent concentration (Thomas and Bloomfield, 1985). Arscott et al. (1995) monitored condensation induced by cobalt (III) hexaammine ($Co(NH_3)6^{3+}$) under conditions that favor the formation of A-DNA in random sequences, and observed a gradual loss of regular condensate morphology. In addition, it was found that the magnitude and sign of supercoiling have observable effects on the architecture of the resulting condensates (Ma and Bloomfield, 1994; Reich et al., 1994). Minsky and co-workers have used these results as evidence for a coupling between DNA sequence and higher order structures that can ultimately regulate cellular parameters (Levin-Zaidman et al., 1996; Reich et al., 1991, 1993).

Telomeric repeat sequences (TRSs), variations of which are found in nearly all eukaryotes, have been shown to exhibit unusual properties both in vivo and in vitro, and are conserved in base composition and orientation. At the ends of yeast chromosomes one finds a short base single-stranded overhang containing the G-rich strand of the telomeric repeat. The G-rich overhangs are able to form unique nonduplex structures in vitro, and relevant biological roles have been proposed (Fang and Cech, 1993; Williamson et al., 1989). An additional 350–400 bp of double-stranded telomeric repeat DNA is packaged into nonnucleosomal structures and is associated with the telomere DNA-binding protein Rap1p (Shore, 1994). Cacchione et al. (1997) have used nucleosome reconstitution studies to show that the nonnucleosomal structure of telomeres may be due, in part, to unfavorable free energies of wrapping the telomeric DNA around the histone core complex. This, in turn, is presumably due to the TRS secondary structure.

Received for publication 25 August 1997 and in final form 14 November 1997.

Address reprint requests to Dr. Victor A. Bloomfield, Department of Biochemistry, University of Minnesota, 1479 Gortner Avenue, St. Paul, MN 55108. Tel.: 612-625-2268; Fax: 612-625-6775; E-mail: victor@maroon.tc.umn.edu.

0006-3495/98/03/1484/08 $2.00

We have used laser light scattering and electron microscopy (EM) to evaluate the effects of inserting a telomeric repeat sequence on the $Co(NH_3)_6^{3+}$-induced condensation of a 3.3-kb plasmid. From EM measurements, we have found that the condensates formed from plasmids containing a 72-bp TRS insert, $(C_{1-3}A)_{13}T(C_{1-3}A)_{12}$, have decreased outer radii, suggesting that growth of the condensates is inhibited. We hypothesize that this inhibition is attributable to incompatible packing geometry of the telomeric repeat DNA with random-sequence DNA.

Total intensity light scattering of the condensed linear plasmids shows a strong dependence on the position of the TRS: the scattering intensity is further depressed when the plasmid is linearized, so that the TRS lies near one of the ends. Furthermore, relative light scattering as a function of $Co(NH_3)_6^{3+}$ shows a transition that is broadened and slightly shifted toward higher $Co(NH_3)_6^{3+}$ concentrations. We hypothesize that in this case there are two components contributing to the decrease in total intensity light scattering. The first, which is seen to a similar extent in the molecules where the TRS lies near the middle, is due to a decrease in the outer radii of the toroidal condensates. The second, which predominates when the TRS is near an end, is a decrease in the total number of condensates due to inhibition of the initiation of condensation.

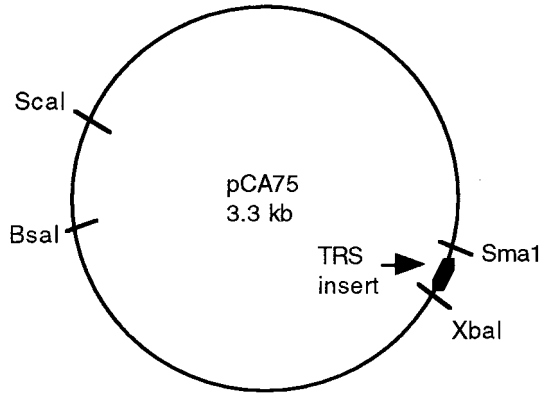

G/GATCCCCCTG**CCACCACACCCACACCACAC**
CCACACCACACCCACAT-CCACACACCCACA
CACCCACACACCCACACCCACCCTCGAGACTA
GAG/GATCC

FIGURE 1 (*Top*) The pCA75 plasmid is a derivative of the pUC-based Bluescribe plasmid (Short et al., 1988). A 95-bp region containing 72 bp of an *S. cerevisiae* telomeric repeat was inserted into the *Bam*HI site (Wellinger et al., 1993). The control plasmid was obtained by digestion with *Bam*HI, gel separation of the fragment lacking the insert, and re-ligation. *Sma*I or *Xba*I restriction endonucleases were used to place the TRS at the end of the resulting linear plasmid; *Sca*I or *Bsa*I placed it at the middle. (*Bottom*) Sequence of insert, with TRS repeat in bold. The cutting site in the *Bam*HI sites (GGATCC) at either end is indicated by /. The bases outside the / are sticky ends left by the cut.

MATERIALS AND METHODS

Materials

Dialysis tubing was purchased from Spectrum. T4 DNA ligase was purchased from Gibco BRL. Agarose was purchased from Pharmacia. Restriction endonucleases were purchased from New England BioLabs, Gibco BRL, or Boehringer Mannheim. Highly purified cobalt (III) hexaammine chloride was purchased from Kodak.

Plasmid DNA

The DNAs are derivatives of the pUC19-based Bluescribe plasmid (Stratagene). The 3332-bp pCA75 plasmid is a derivative of pVZ1 (Henikoff and Eghtedarzadeh, 1987) with a 95-bp region inserted into the *Bam*HI site. The insert comprises 72 bp of telomeric repeat cloned from *Saccharomyces cerevisiae*, and an additional 23 bp of flanking DNA (Wellinger et al., 1993). Its sequence is shown in Fig. 1.

The control plasmid, pHC1, was obtained by complete digestion of pCA75 with *Bam*HI, gel isolation of the DNA band lacking the TRS insert, and re-ligation by T4 ligase. Removal of the insert was verified by DNA sequencing.

Plasmid preparation

Plasmids were propagated in *Escherichia coli* (DH5a or XL-1 Blue) on Luria-Bertani media (Sambrook et al., 1989). Plasmid DNA was isolated and purified by a previously developed procedure (Baumann and Bloomfield, 1995). Linear plasmids were obtained by extracting the digest solution with phenol saturated with TE buffer (10 mM Tris-Cl, 1 mM EDTA, pH 8.0), extensively dialyzing in 25-kDa dialysis tubing against TE, precipitating with 5 M NaCl and ethanol, and resuspending in TE that had been filtered through 0.2-μm filters (Millipore). DNA stock concentrations were determined spectrophotometrically: a solution with $OD_{260} = 1$ was taken to be 50 μg/ml. Sample purity was verified by $A_{260}/A_{270} \geq 1.22$ and $2.00 \geq A_{260}/A_{280} \geq 1.85$.

Light scattering

Total intensity light scattering experiments were performed as described previously (Ma et al., 1995), with the following modifications. As before, a Lexel argon ion laser operating at 488 nm impinged on a sample held in a borosilicate glass cuvette. The scattering at 90° was fed directly from the PMT to a model BI-9000AT digital correlator (Brookhaven Instruments Corporation). Total scattering intensity of condensed DNA relative to that of the uncondensed DNA was monitored at 90° as a function of time after the addition of $Co(NH_3)_6^{3+}$. Unless otherwise indicated, all condensation experiments were done with 5 μg/ml DNA and 30 μM $Co(NH_3)_6^{3+}$. Plots of scattering versus time represent the average of three separate runs.

Electron microscopy

Samples for electron microscopy were prepared as described previously (Arscott et al., 1990). Samples were viewed on a Philips CM-12 TEM at 45,000× and recorded either on photographic negatives or via a CCD camera inserted into the TEM column. Images were then scanned into NIH Image and digitized for measurement of toroid dimensions.

Fragment DNA

The 95-bp fragment containing 72-bp of telomeric repeat was isolated from pCA75 digested with *Bam*HI. For a control, a 105-bp random sequence fragment was obtained by digestion of pHC1 with the restriction endonuclease *Bsp*HI. The fragments were isolated by excision of the correspond-

ing bands on an agarose gel. The samples were purified by extraction with TE-saturated phenol and extensively dialyzed against 1 × TE.

Circular dichroism

CD spectra were collected on a Jasco 710 spectrometer at room temperature. Samples were held in 1-cm-pathlength cells, and DNA concentrations were 5 μg/ml, as in total intensity light scattering experiments. Spectra of solutions without DNA were taken as baselines and subtracted from the final DNA spectra.

RESULTS

To evaluate the effects of the telomeric $C_{1-3}A$ repeat on the cation-induced condensation of plasmid DNA, we used the complementary techniques of total intensity light scattering and EM to monitor the condensation of a plasmid with and without a TRS insert. As a plasmid DNA undergoes condensation from an expanded coil to a compact form, the DNA behaves more like a point scatterer, allowing a larger portion of the scattered light to reach the detector. Monitoring the light scattered after the addition of a condensing agent provides a simple measurement of the extent of condensation (Wilson and Bloomfield, 1979). The pCA75 plasmid (3.3 kb) contains a 72-bp TRS inserted into the *Bam*HI site plus 23 bp of flanking DNA. The control plasmid pHC1 was made by simply cutting pCA75 with the *Bam*HI restriction endonuclease and re-ligating.

Four restriction endonucleases were used to produce plasmids linearized at various distances from the TRS insert site (Fig. 1). Linearizing with *Sma*I or *Xba*I produced plasmids with the TRS approximately 10 bp from the end of the plasmid, but with different orientations. Digestion with *Sma*I generated a fragment with TRS orientation like that found at the chromosomal termini, with the G-rich strand running 5' to 3' toward the end of the molecule. Cutting with *Bsa*I or *Sca*I placed the TRS near the middle of the linearized plasmid. The enzymes also yield different types of cut ends: *Xba*I and *Bsa*I produce 5' overhangs, whereas *Sma*I and *Sca*I produce blunt ends. All condensation experiments were done with 5 μg/ml of plasmid DNA. Condensation was induced by the addition of 30 μM $Co(NH_3)_6^{3+}$, and the progress was monitored by total intensity light scattering (Fig. 2). In every case, insertion of the 95-bp fragment containing the telomeric repeat sequence decreased the condensation, as monitored by total intensity light scattering.

The extent to which the condensation was depressed upon insertion of the TRS depended on the position of the TRS within the linearized plasmid. Linearization of pCA75,

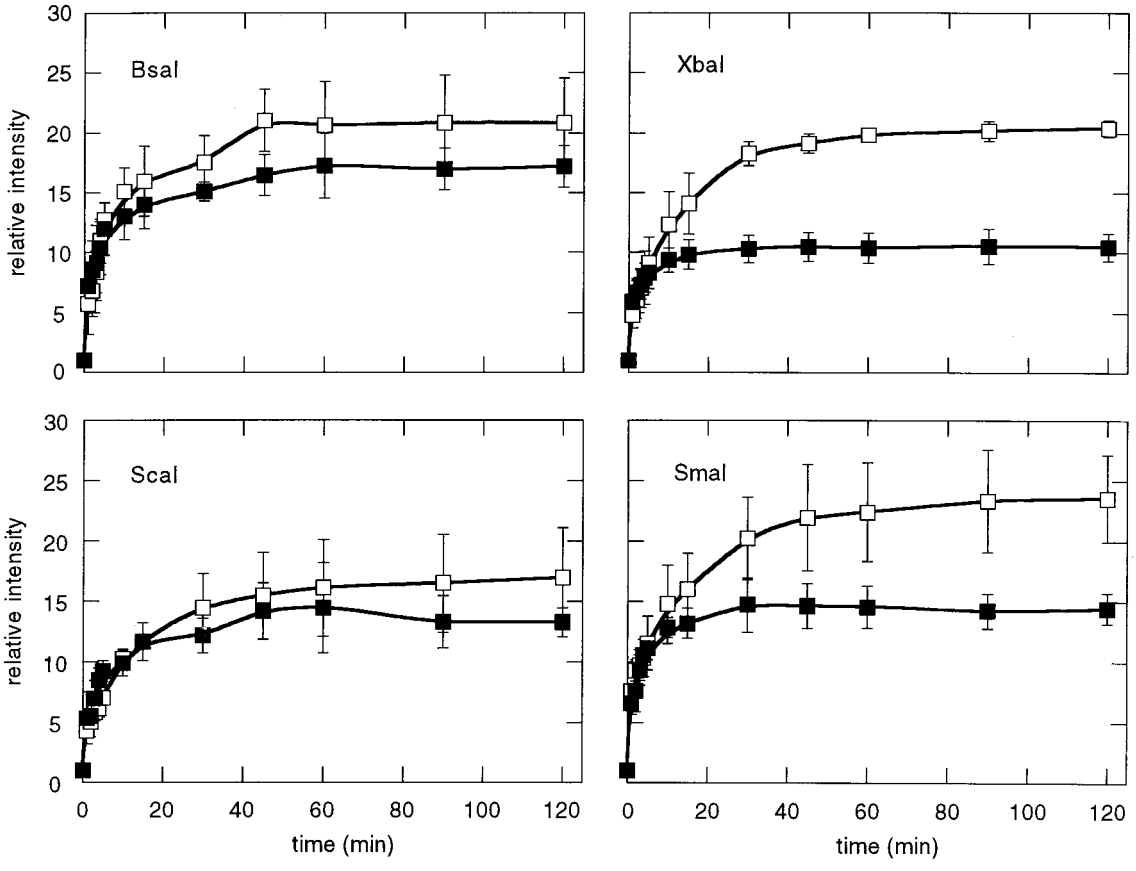

FIGURE 2 Relative total scattering intensity of the linearized plasmids pHC1 (□) and pCA75 (■) as a function of time after the addition of $Co(NH_3)_6^{3+}$. (*Left*) Plasmids cut with enzymes that place the TRS insert site at the middle. (*Right*) Plasmids cut with enzymes that place the TRS insert site near an end. (*Top*) Enzymes that leave 5'overhangs. (*Bottom*) Enzymes that leave blunt ends. Error bars indicate the standard deviation of three separate experiments.

which placed the TRS near the middle, led to a decrease in light scattering of 18–22% (Fig. 2, *left*). In contrast, linearization that placed the TRS near one of the ends resulted in a decrease in condensation by 39–49% (Fig. 2, *right*). The 5' overhang cutter *Bsa*I appears to produce slightly higher scattering than the blunt cutter *Sca*I, perhaps because of some end-to-end association of single-stranded overhangs.

Electron microscopy

The intensity of light scattered at a given angle from a solution of toroids, like any macromolecular particle, depends primarily on the number and size of the toroids (Bloomfield et al., 1974). EM was done after the condensation experiments to determine the size of the toroids (Table 1). Typical images are shown in Fig. 3. The mean values from the measurement of inner and outer toroidal radii showed a significant decrease of nearly 30 Å in the outer radii of the toroids produced from pCA75. The inner radii changed negligibly. The result was a 22% decrease in toroid thickness. According to these measurements, the toroids with TRS inserts contain, on average, two or three plasmids, whereas those without inserts contain three or four. (These are estimates, given our lack of knowledge of the *z* axis dimensions of the two populations.) This only partially explains the decrease in light scattering observed in Fig. 1, because a change in toroid size did not accompany the larger decrease in light scattering observed when the TRS was near one of the ends (compare R_{in} and R_{out} for pCA75 in Table 1).

It is worth noting that although the TRS insert leads to a 22% decrease in thickness, the insert comprises only 2.85% of the DNA base pairs. Therefore, the shrinkage in dimensions is not due to the different physical-chemical properties of the TRS or its junctions with normal DNA.

$Co(NH_3)_6^{3+}$ titration

Using a rapid mixing technique, it has been shown by EM that the formation of a toroid from plasmid DNA occurs from the inside out, i.e., the inner radius is formed initially (Christoph Baumann, personal communication). The decrease in the outer radii observed here suggests that the TRS somehow inhibits the growth of the toroids. To explore the possibility that the TRS-containing plasmids simply require a higher concentration of condensing agent, a series of titration experiments was carried out. The total intensity light scattering of the condensed DNA solutions was recorded as a function of condensing agent concentration for the linearized plasmids. The results, shown in Fig. 4, suggest that when the TRS was near the end of the linearized plasmid (cut with *Sma*I or *Xba*I), the transition from extended to condensed was shifted to slightly higher $Co(NH_3)_6^{3+}$ concentrations, and the change in scattering intensity was less dramatic. A decreased level of scattering was observed for the TRS-containing plasmids at nearly all concentrations of $Co(NH_3)_6^{3+}$ used, indicating that a shift in the critical condensing agent concentration was not responsible for the changes observed in EM or total intensity light scattering. At high $Co(NH_3)_6^{3+}$ concentrations, the 5' overhang cutters *Bsa*I and *Xba*I give consistently higher scattering intensities than the blunt cutters *Sca*I and *Sma*I, suggesting a tendency for association of single-stranded ends under these strong condensing conditions.

TABLE 1 EM measurements of toroidal condensates

Enzyme	# measured	R_{out} (Å)	R_{in} (Å)	R_{out}-R_{in} (Å)	TRS*
pCA75					
*Sca*I	223	241 ± 40	112 ± 30	129	Middle
*Bsa*I	79	238 ± 25	127 ± 22	111	Middle
*Xba*I	143	257 ± 35	143 ± 28	114	End
*Sma*I	169	252 ± 30	134 ± 22	118	End
Mean ± SD		247 ± 34	127 ± 28	120	
pHC1					
*Sca*I	65	299 ± 37	129 ± 30	170	Middle
*Bsa*I	98	248 ± 25	103 ± 22	145	Middle
*Xba*I	134	293 ± 38	138 ± 24	155	End
*Sma*I	201	269 ± 44	119 ± 30	150	End
Mean ± SD		275 ± 42	122 ± 30	153	

*Position of the TRS upon linearization at the indicated restriction enzyme site.

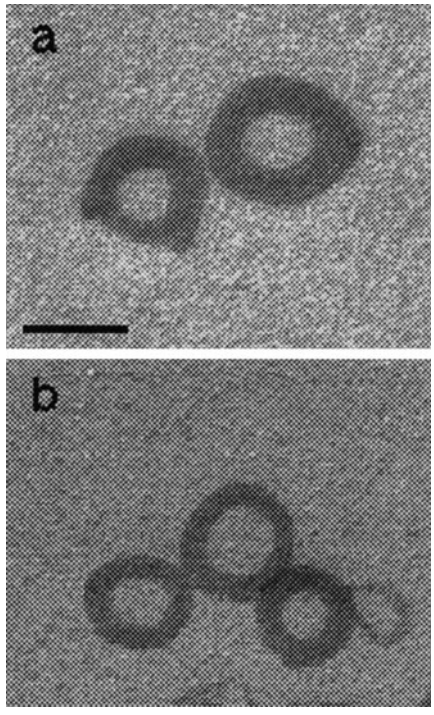

FIGURE 3 Electron micrographs of typical toroids produced by condensation of linearized plasmids in 30 μM $Co(NH_3)_6^{3+}$. (*a*) pHC1. (*b*) pCA75. Scale bar represents 500 Å.

Circular dichroism

Circular dichroism (CD) of the 95-bp fragment containing the 72 bp of yeast TRS (Fig. 5) suggests a right-handed

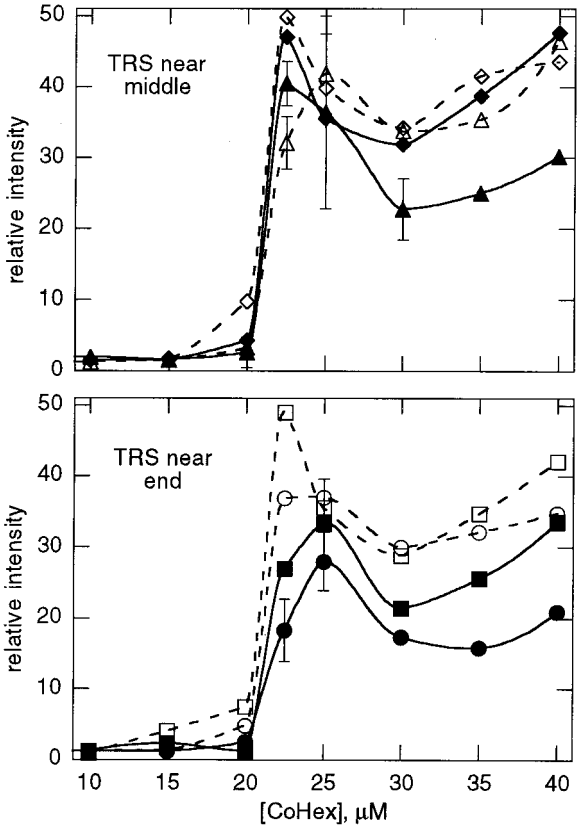

FIGURE 4 Relative total scattering intensity 2 h after the addition of $Co(NH_3)_6^{3+}$ to pHC1 (*dashed line, open symbols*) or pCA75 (*solid line, filled symbols*). (*Top*) TRS near the middle of plasmids linearized at (◇) *Bsa*I or (△) *Sca*I sites. (*Bottom*) TRS near the end of plasmids linearized at (○) *Sma*I or (□) *Xba*I sites. All solutions contained 5 μg/ml DNA. Error bars are given for data points where two or three experiments were performed and represent typical standard deviations.

duplex both in the presence and the absence of $Co(NH_3)_6^{+}$. The CD spectrum of the fragment bears little resemblance to that expected for a tetraplex structure (Balagurumoorthy et al., 1992; Giraldo et al., 1994). The CD spectrum of the control fragment appears to be consistent with previously published B-form spectra (Sprecher et al., 1979). The deviations seen with the telomeric repeat spectra are similar to those of DNAs intermediate between the A-form and B-form (Fairall et al., 1989; Huber et al., 1991): an increase in magnitude of the positive peak centered at around 270 nm, a decrease in magnitude of the negative ellipticity at 245 nm, and a shifting of the peaks and the cross-over point by ~5–15 nm.

DISCUSSION

The trends in DNA condensation monitored by total intensity light scattering and electron microscopy suggest that the TRS possesses unique packing properties within the condensed particle. The presence of the 72-bp TRS results in a decrease in thickness of the toroidal condensates due to a reduced outer radius, indicating that accumulation of additional turns of DNA around the initial nucleus is disfavored by some structural property of the TRS. Circular dichroism, and other evidence discussed below, suggest that this structural property may be an A-like secondary structure, leading to unfavorable packing with the surrounding B-form DNA.

Secondary structure of the telomeric repeat sequence

The GC-rich composition (64%) and G-tract/C-tract nature of the telomeric repeat are likely a significant determinant of its unique secondary structure and condensation properties. Although solution studies of DNA often indicate a B-form helix regardless of sequence and composition, crystallization or introduction of high salt concentrations can induce changes to A- or Z-form (Wahl and Sundaralingam, 1997). These changes are sensitive to the presence of particular dinucleotide and trinucleotide steps. In the case of A-form DNA, one finds that two or more G · C or C · G basepairs in a row leads to a propensity for A-form in dehydrating conditions and/or high salt solutions. (Minchenkova et al., 1986; Wahl and Sundaralingam, 1997).

Both fiber diffraction and solution studies have shown that stretches of guanine residues will favor the A-form helix under appropriate conditions of salt and hydration (Minchenkova et al., 1986; Robinson and Wang, 1996). Nishimura et al. (1985) have observed the B-A transition in poly(dG) · poly(dC) at high nucleotide concentrations in aqueous solution using Raman spectroscopy. In addition, multivalent cations such as spermine and $Co(NH_3)_6^{3+}$ have been shown to bind specifically to guanine residues and promote the B-A transition (Braunlin and Xu, 1992; Xu et al., 1993). Arscott et al. (1995) have observed synergistic effects of $Co(NH_3)_6^{3+}$ on the ability of alcohols to induce the A conformation in random-sequence DNA.

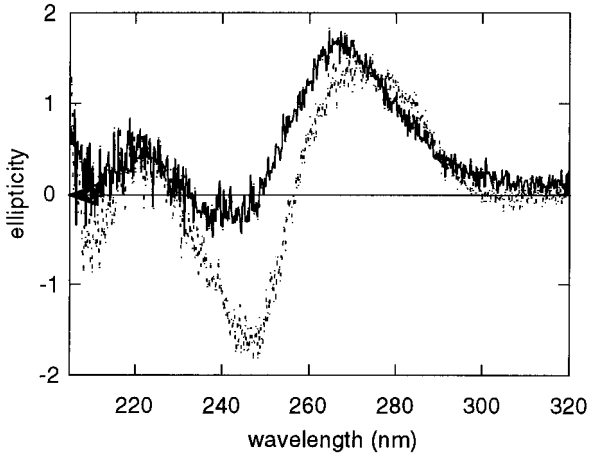

FIGURE 5 Circular dichroism of TRS insert excised from pCA75 (*dark trace*) and random sequence fragment of similar size for comparison (*light trace*). Solution conditions were 5 μg/ml DNA, 1 mM NaCl, 1 mM Na cacodylate, 0.1 × TE buffer, pH 7.0.

The TRS likely has a propensity for the A-form because of its sequence peculiarities. Our CD measurements suggest that the TRS may already be in a form intermediate between A-form and B-form in dilute solution. Under our experimental conditions, condensation results in a high local concentration of DNA and $Co(NH_3)_6^{3+}$, which may induce a full conversion of the TRS to the A-form helical structure.

The idea that the TRS has an A-like structure is reinforced by the similarity of the TRS to other sequences whose structure has been determined to have A-form characteristics. A prominent example is the transcription factor IIIA (TFIIIA) consensus core binding site d(GGATGGGAG) · d(CTCCCATCC) (Brown, 1982, and references therein). This sequence has comparable GC content (67% versus 64% for TRS) and GpG base-pair step frequency. X-ray crystallography (McCall et al., 1986) and nuclease digestion (Budarf and Blackburn, 1987) suggest an underwound structure similar to the A-form for the TFIIIA binding site. Another example is found in the GLI protein-binding site, which contains a 9-bp region very similar to the yeast TRS. In the crystal structure of the full 18-bp binding site complexed with GLI protein, the 9 bp d(ACCACCCAA) · d(TTGGGTGGT) exhibit characteristics intermediate between A-form and B-form, whereas the rest of the site remains in B-form (Pavletich and Pabo, 1993).

Finally, we note that it is likely that the interior of a toroid has more in common with the tight packing and reduced solvation of DNA in a fibrous or crystalline milieu—conditions favorable to the A conformation—than with conditions in free solution (Schellman and Parthasarathy, 1984).

Packing of the TRS

Although packing inside a condensed DNA toroid has not been observed directly at atomic resolution, it seems reasonable that close, essentially parallel alignment of adjacent double helices is necessary to achieve the requisite tight packing. Such alignment is apparent in freeze-etch electron micrographs of hydrated DNA toroids (Marx and Ruben, 1983). It is therefore relevant to note the observation by Wahl and Sundaralingam (1997) that different DNA structural classes tend to have distinct crystallization patterns. For example, B-form DNAs tend to pack uniformly with the solvent, whereas in A-form crystals the DNA and solvent are often seen to segregate, with the helices packed tightly together, leaving a large channel of solvent. This highlights the importance of DNA secondary structure on higher order interactions (Reich et al., 1991; Wahl and Sundaralingam, 1997).

If the condensate interior is a highly regular array of DNA helices, then the compatibility of the helical geometry will play a role in condensate stability. Circular dichroism of condensed DNA suggests that it remains predominantly in B-form (Gosule and Schellman, 1978; Wilson and Bloomfield, 1979). Packing a unique TRS secondary structure into a primarily close-packed B-form environment with only an 8 Å surface-to-surface distance (Rau and Parsegian, 1992; Schellman and Parthasarathy, 1984) would be unfavorable. The incompatible geometry would disrupt the interactions of adjacent DNAs, decreasing the energetic rewards of the condensed state. Additional incorporation of the incompatible DNA structure would then be avoided at the expense of condensate growth.

Effect of TRS position on toroid nucleation and growth

Recent experimental and theoretical results suggest that, in the coil-to-globule transition of linear polymers, nucleation of collapse does not occur with equal probability at all points along the chain. Direct observation of the collapse of single DNA molecules by fluorescence microscopy shows that collapse is initiated near the ends of the linear molecule ~70% of the time (Matsuzawa et al., 1996). Simulations (Ostrovsky and Bar-Yam, 1994) of the coil-to-globule transition of model polymers also predict that collapse is not uniform along the length of the polymer, but rather starts preferentially at the ends.

Nucleation at a TRS-containing end may be particularly favored because of the preference of the condensing agent $Co(NH_3)_6^{3+}$ to bind to stretches of guanines. Another factor that may favor nucleation in TRS regions is the prevalent trinucleotide motif CAC. Lu et al. (1985) have compiled a list of DNA sites at which proteins interact, and found the CAC motif to be strongly overrepresented. It has been suggested that the flexibility of CA repeats at the centers of binding sites facilitates protein-induced bending (Lyubchenko et al., 1993). This flexibility may offset the rigidity of the posited A-form stretch of DNAs and facilitate end diffusion, leading to the formation of a nucleation core.

Combining these ideas, we are led to speculate that the TRS, when positioned at the ends of a DNA molecule, has significant probability of forming an abortive nucleation core because of its distinctive packing geometry. Once the TRS forms the initial core, either subsequent association of B-form DNA is less favored, or the association of other TRS strands traps the complex and does not allow normal toroid formation. The decrease in light scattering when the TRS is near the end of a molecule is then due to a decrease in the number of condensed particles as well as a reduction in toroid thickness. However, if the nucleation is productive, our EM data indicate that there is little difference in size between toroids that are formed with the TRS in the middle or at an end of the DNA.

DNA condensation as a probe of conformational variation

Aside from its unusual CD spectrum, the TRS fragment shows no unusual physical features. We assayed the electrophoretic mobility of the 95-bp fragment containing 72 bp of TRS on a 20% polyacrylamide gel (data not shown) and detected no anomalous mobility, which suggests no se-

quence-directed bending. Thus in vitro DNA condensation may provide a unique indicator of otherwise hard-to-observe phenomena arising from sequence and composition, including stiffness, geometry, and phasing.

We are grateful to Maryam Gerami-Nejad and Dr. Miriam Gulotta for technical assistance and useful discussions. This research was supported in part by research grants NIH GM28093 and NSF MCB 9418053 to VAB, and NIH GM38626, NSF MCB 9205997, and CTR 4061 to JB.

REFERENCES

Arscott, P. G., A.-Z. Li, and V. A. Bloomfield. 1990. Condensation of DNA by trivalent cations. 1. Effects of DNA length and topology on the size and shape of condensed particles. *Biopolymers.* 30:619–630.

Arscott, P. G., C. Ma, J. R. Wenner, and V. A. Bloomfield. 1995. DNA condensation by cobalt hexaammine(III) in alcohol-water mixtures: dielectric constant and other solvent effects. *Biopolymers.* 36:345–364.

Balagurumoorthy, P., S. K. Brahmachari, D. Mohanty, M. Bansal, and V. Sasisekharan. 1992. Hairpin and parallel quartet structures for telomeric sequences. *Nucleic Acids Res.* 20:4061–4067.

Baumann, C. G., and V. A. Bloomfield. 1995. Large-scale purification of plasmid DNA for biophysical and molecular biology studies. *BioTechniques.* 19:884–886.

Bloomfield, V. A. 1996. DNA condensation. *Curr. Opin. Struct. Biol.* 6:334–341.

Bloomfield, V. A., D. M. Crothers, and I. Tinoco, Jr. 1974. Physical Chemistry of Nucleic Acids. Harper and Row, New York.

Braunlin, W. H., and Q. Xu. 1992. Hexaamminecobalt(III) binding environments on double-helical DNA. *Biopolymers.* 32:1703–1711.

Brown, D. D. 1982. How a simple animal gene works. *Harvey Lect.* 76:27–44.

Budarf, M., and E. Blackburn. 1987. S1 nuclease sensitivity of a double-stranded telomeric DNA sequence. *Nucleic Acids Res.* 15:6273–6292.

Cacchione, S., M. A. Cerone, and M. Savino. 1997. In vitro low propensity to form nucleosomes of four telomeric sequences. *FEBS Lett.* 400: 37–41.

Duguid, J. G., V. A. Bloomfield, J. M. Benevides, and G. J. Thomas. 1995. Raman spectroscopy of DNA-metal complexes. II. The thermal denaturation of DNA in the presence of Sr^{2+}, Ba^{2+}, Mg^{2+}, Ca^{2+}, Mn^{2+}, Co^{2+}, Ni^{2+}, and Cd^{2+}. *Biophys J.* 69:2623–2641.

Fairall, L., S. Martin, and D. Rhodes. 1989. The DNA binding site of the *Xenopus* transcription factor IIIA has a non-B-form structure. *EMBO J.* 8:1809–1817.

Fang, G., and T. R. Cech. 1993. The β-subunit of Oxytricha telomere-binding protein promotes G-quartet formation by telomeric DNA. *Cell.* 74:875–885.

Giraldo, R., M. Suzuki, L. Chapman, and D. Rhodes. 1994. Promotion of parallel DNA quadruplexes by a yeast telomere binding protein: a circular dichroism study. *Proc. Natl. Acad. Sci. USA.* 91:7658–7662.

Gosule, L. C., and J. A. Schellman. 1976. Compact form of DNA induced by spermidine. *Nature.* 259:333–335.

Gosule, L. C., and J. A. Schellman. 1978. DNA condensation with polyamines. I. Spectroscopic studies. *J. Mol. Biol.* 121:311–326.

Henikoff, S., and M. K. Eghtedarzadeh. 1987. Conserved arrangements of nested genes at the *Drosophila Gart* locus. *Genetics.* 117:711–725.

Huber, P. W., G. C. Blobe, and K. M. Hartmann. 1991. Conformational studies of the nucleic acid binding sites for *Xenopus* transcription factor IIIA. *J. Biol. Chem.* 266:3278–3268.

Levin-Zaidman, S., Z. Reich, E. J. Wachtel, and A. Minsky. 1996. Flow of structural information between four DNA conformational levels. *Biochemistry.* 35:2985–2991.

Lu, P., S. Cheung, and M. Donlan. 1985. A recurrent DNA sequence at sites of protein interaction. *Adv. Biophys.* 20:153–175.

Lyubchenko, Y. L., L. S. Shlyakhtenko, E. Appella, and R. E. Harrington. 1993. CA runs increase DNA flexibility in the complex of lambda Cro protein with the OR3 site. *Biochemistry.* 32:4121–4127.

Ma, C., and V. A. Bloomfield. 1994. Condensation of supercoiled DNA induced by $MnCl_2$. *Biophys. J.* 67:1678–1681.

Ma, C., L. Sun, and V. A. Bloomfield. 1995. Condensation of plasmids enhanced by Z-DNA conformation of d(CG)n inserts. *Biochemistry.* 34:3521–3528.

Marx, K. A., and G. C. Ruben. 1983. Evidence for hydrated spermidine-calf thymus DNA toruses organized by circumferential DNA wrapping. *Nucleic Acids Res.* 11:1839–1854.

Matsuzawa, Y., Y. Yonezawa, and K. Yoshikawa. 1996. Formation of nucleation center in single double-stranded DNA chain. *Biochem. Biophys. Res. Commun.* 225:796–800.

McCall, M., T. Brown, W. N. Hunter, and O. Kennard. 1986. The crystal structure of d(GGATGGGAG) forms an essential part of the binding site for transcription factor IIIA. *Nature.* 322:661–664.

Minchenkova, L. E., A. K. Schyolkina, B. K. Chernov, and V. I. Ivanov. 1986. CC/GG contacts facilitate the B to A transition of DNA in solution. *J. Biomol. Struct. Dyn.* 4:463–476.

Nishimura, Y., C. Torigoe, and M. Tsuboi. 1985. An A-form poly(dG) · poly(dC) in H_2O solution. *Biopolymers.* 24:1841–1844.

Ostrovsky, B., and Y. Bar-Yam. 1994. Irreversible polymer collapse in 2 and 3 dimensions. *Europhys. Lett.* 25:409–414.

Pavletich, N. P., and C. O. Pabo. 1993. Crystal structure of a five-finger GLI-DNA complex: new perspectives on zinc fingers. *Science.* 261: 1701–1707.

Plum, G. E., P. G. Arscott, and V. A. Bloomfield. 1990. Condensation of DNA by trivalent cations. 2. Effect of cation structure. *Biopolymers.* 30:631–643.

Rau, D. C., and V. A. Parsegian. 1992. Direct measurement of the intermolecular forces between counterion-condensed DNA double helices. Evidence for long range attractive hydration forces. *Biophys. J.* 61: 246–259.

Reich, Z., P. Friedman, S. Levin-Zaidman, and A. Minsky. 1993. Effects of adenine tracts on the B-Z transition. Fine tuning of DNA conformational transition processes. *J. Biol. Chem.* 268:8261–8266.

Reich Z., R. Ghirlando, and A. Minsky. 1991. Secondary conformational polymorphism of nucleic acids as a possible functional link between cellular parameters and DNA packaging processes. *Biochemistry.* 30: 7828–7836.

Reich, Z., R. Ghirlando, and A. Minsky. 1992. Nucleic acids packaging processes: effects of adenine tracts and sequence-dependent curvature. *J. Biomol. Struct. Dyn.* 9:1097–1109.

Reich, Z., S. Levin-Zaidman, S. B. Gutman, T. Arad, and A. Minsky. 1994. Supercoiling-regulated liquid-crystalline packaging of topologically-constrained, nucleosome-free DNA molecules. *Biochemistry.* 33: 14177–14184.

Robinson, H., and A. H. J. Wang. 1996. Neomycin, spermine and hexaamminecobalt(III) share common structural motifs in converting B- to A-DNA. *Nucleic Acids Res.* 24:676–682.

Sambrook, J., E. F. Fritsch, and T. Maniatis. 1989. Molecular Cloning: A Laboratory Manual, Vol. 3, 2nd Ed. Cold Spring Harbor Laboratory, Cold Spring Harbor, NY.

Schellman, J. A., and N. Parthasarathy. 1984. X-ray diffraction studies on cation-collapsed DNA. *J. Mol. Biol.* 175:313–329.

Shore, D. 1994. RAP1: protean regulator in yeast. *Trends Genet.* 10: 408–412.

Short, J. M., J. M. Fernandez, J. A. Sorge, and W. D. Huse. 1988. Lambda ZAP: a bacteriophage lambda expression vector with in vivo excision properties. *Nucleic Acids Res.* 16:7583–7600.

Sprecher, C. A., W. A. Baase, and W. C. Johnson, Jr. 1979. Conformation and circular dichroism of DNA. *Biopolymers.* 18:1009–1019.

Thomas, T. J., and V. A. Bloomfield. 1983. Collapse of DNA caused by trivalent cations: pH and ionic specificity effects. *Biopolymers.* 22: 1097–1106.

Thomas, T. J., and V. A. Bloomfield. 1984. Ionic and structural effects on the thermal helix-coil transition of DNA complexed with natural and synthetic polyamines. *Biopolymers.* 23:1295–1306.

Thomas, T. J., and V. A. Bloomfield. 1985. Toroidal condensation of Z DNA and identification of an intermediate in the B to Z transition of poly(dG-m^5dC) · poly(dG-m^5dC). *Biochemistry.* 24:713–719.

Wahl, M. C., and M. Sundaralingam. 1997. Crystal structures of A-DNA duplexes. *Biopolymers.* 44:45–63.

Wellinger, R. J., A. J. Wolf, and V. A. Zakian. 1993. Saccharomyces telomeres acquire single-strand TG1–3 tails late in S phase. *Cell.* 72: 51–60.

Widom, J., and R. L. Baldwin. 1980. Cation-induced toroidal condensation of DNA: studies with $Co^{3+}(NH_3)_6$. *J. Mol. Biol.* 144:431–453.

Widom, J., and R. L. Baldwin. 1983. Monomolecular condensation of λ-DNA induced by cobalt hexaammine. *Biopolymers.* 22:1595–1620.

Williamson, J. R., M. K. Raghuraman, and T. R. Cech. 1989. Monovalent cation-induced structure of telomeric DNA: the G-quartet model. *Cell.* 59:871–880.

Wilson, R. W., and V. A. Bloomfield. 1979. Counterion-induced condensation of deoxyribonucleic acid. A light-scattering study. *Biochemistry.* 18:2192–2196.

Xu, Q., R. K. Shoemaker, and W. H. Braunlin. 1993. Induction of B-A transitions of deoxyoligonucleotides by multivalent cations in dilute aqueous solution. *Biophys. J.* 65:1039–1049.